Nonlinear Dyn (2014) 78:317–327
DOI 10.1007/s11071-014-1441-y

ORIGINAL PAPER

Chaos control in a pendulum system with excitations and phase shift

Xianwei Chen · Zhujun Jing · Xiangling Fu

Received: 21 February 2013 / Accepted: 29 April 2014 / Published online: 21 May 2014

Abstract Melnikov methods are used for suppressing homoclinic and heteroclinic chaos of a pendulum system with a phase shift and excitations. This method is based on the addition of adjustable amplitude and phase-difference of parametric excitation. Theoretically, we give the criteria of suppression of homoclinic and heteroclinic chaos, respectively. Numerical simulations are given to illustrate the effect of the chaos control in this system. Moreover, we calculate the maximum Lyapunov exponents (LEs) in parameter plane, and study how to vary the maximum LE when the parametric frequency varies.

X. Chen (✉) · X. Fu
School of Mathematics and Computational Science,
Hunan University of Science and Technology,
Xiangtan 411201, People's Republic of China
e-mail: chenxianwei11@aliyun.com

X. Fu
e-mail: fxl8923@126.com

X. Chen · Z. Jing
College of Mathematics and Computer Science ,
Key Laboratory of High Performance Computing and
Stochastic Information Processing (Ministry of Education
of China), Hunan Normal University,
Changsha 410081, Hunan, People's Republic of China

Z. Jing
Academy of Mathematics and Systems Science,
Chinese Academy of Sciences, Beijing 100190,
People's Republic of China

Keywords Pendulum equation · Phase shift · Bifurcation · Chaos control · Melnikov methods

1 Introduction

Plenty of academic research about controlling chaos and bifurcations have been studied after the pioneering works of OGY [20,22]. For example, Chen et al. [9,10] and Kapitaniak [15] introduced recent developments in the fields of controlling chaos and bifurcations, an optimal control method developed by Lenci and Rega [16–18] has been applied to various nonlinear oscillators, and so on. It is well known that homoclinic and heteroclinic bifurcation is a kind of important source of structural instabilities in nonlinear dynamical systems. The chaotic dynamics are usually derived from the homoclinic or heteroclinic intersection between the stable and unstable manifolds in the Poincaré map. So homoclinic and heteroclinic bifurcation can not be ignored in most cases, consequently the elimination or suppression of chaotic dynamics is desirable from a practical point of view. Chacón proposed Melnikov methods in [6–8]. Cao and Chen [4] used Melnikov methods to study the suppression of homoclinic and heteroclinic bifurcation of a general one-degree-of-freedom nonlinear oscillator. Cao et al. [3] used weak resonant excitations to control choas in an externally-forced froude pendulum. Wang et al. [23], Yang and Jing [27] studied the pendulum equation by using Melnikov methods, and gave the conditions of suppression of homoclinic and heteroclinic chaos. Research on controlling chaos of pendulum equation can be seen in references [1,2,5,21,25,26]. We will use Melnikov methods to study the pendulum equation with excitations and a phase shift in this paper.

We consider the problem of suppressing chaos of the following pendulum equation with a phase shift and excitations

$$\dot{x} = y, \quad \dot{y} = -\alpha x - \delta y - [1 + f_0 \cos(\Omega t + \Psi)] \sin x + f_1 \sin(\omega t + \theta), \tag{1}$$

where δ is the damping constant, α represents the spring constant, $f_1 \sin(\omega t + \theta)$ is the external excitations for driving the system to chaotic state, θ denotes the phase shift, parametric excitation $f_0 \cos(\Omega t + \Psi)$ is the chaos-suppressing excitation.

The chaotic behavior of system (1) for some special cases has been extensively studied, for examples, for $\alpha = 0, \theta = 0$, and $f_0 = 0$, D'Humieres et al. [12] gave an experimental study of the chaotic states and shown the symmetry breaking of periodic orbits, intermittent behavior,and period-triple bifurcations in chaotic region. Wiggins [24] and Nayfeh and Mook [19] investigated the existence of the chaotic dynamics of the system (1) for $f_0 = 0$ and $\theta = 0$ by using Melnikov function. Jing and Yang [13,14] studied the bifurcation of periodic solution and criterions of existence of chaos for system (1) as $\Psi = 0$ and $\theta = 0$ under periodic and quasi-periodic perturbation by using Melnikov function and second-order averaging method and numerical simulations. Yang and Jing [27] researched the inhibition of chaos of the system (1) for $\theta = 0$ by using Melnikov methods proposed in [7]. Chen and Jing [11] studied the bifurcation of periodic solution and criterions of existence of chaos for system (1) as $\Psi = 0$ under periodic and quasi-periodic perturbation by using Melnikov function, second-order averaging method, and numerical simulations. However, there has been less attention to the inhibition of chaos for the pendulum equation (1) with excitations and a phase shift.

In this paper, Melnikov methods [7] are used for suppressing homoclinic and heteroclinic chaos of a pendulum system with a phase shift and excitations. By computing Melnikov function, we give the conditions of existence of homoclinic and heteroclinic chaos, respectively. Using Melnikov methods proposed in [7], we obtain the corresponding criteria of suppression of homoclinic and heteroclinic chaos for primary and subharmonic resonance ($\Omega/\omega = p/1,\ p \in N^+$), respectively. Numerical simulations are given to illustrate the effect of the chaos control in this system. Moreover, we calculate the maximum Lyapunov exponents (LEs) in parameter plane, and study how to vary the maximum LE when the parametric frequency varies.

The organization of the paper is as follows. In Sect. 2, we provide the fixed points and phase portraits for the unperturbed system of system (1) for showing the existence of homoclinic orbit and heteroclinic orbit. In Sect. 3, we get the conditions of existence of homoclinic and heteroclinic chaos by computing Melnikov function. In Sect. 4, by using Melnikov methods proposed in [7], suitable initial phase-difference intervals and parameter intervals for controlling chaos are studied, and the criteria for suppression of the homoclinic and heteroclinic chaos are given, respectively. In Sect. 5, we give numerical simulation, numerical simulations show the consistency and difference with the theoretical analysis. The conclusion is given in Sect. 6.

2 Fixed points and phase portraits for unperturbed system

When $\delta = f_0 = f_1 = 0$, the system (1) becomes

$$\dot{x} = y, \quad \dot{y} = -\sin x - \alpha x, \tag{2}$$

which is considered as an unperturbed system.

The unperturbed system (2) is a Hamiltonian system, the corresponding Hamiltonian function is given as

$$H(x,\ y) = \frac{1}{2}y^2 + 1 - \cos x + \frac{\alpha}{2}x^2, \tag{3}$$

and potential function is

$$V(x,\ y) = 1 - \cos x + \frac{\alpha}{2}x^2. \tag{4}$$

Jing and Yang [13] give the analysis of the fixed points and their stabilities for system (2), we can find the following Lemma in paper [13].

Lemma 1 [13]

(i) *For $\alpha = 0$, there are infinite fixed points $(K\pi,\ 0)$, where $K \in N$, and $(K\pi,\ 0)$ are centers for K even, saddle for K odd.*

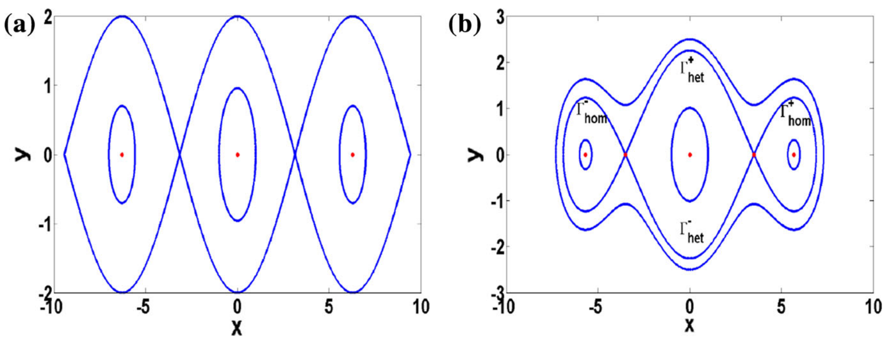

Fig. 1 Phase portrait of system (2): **a** for $\alpha = 0$; **b** for $\alpha = 0.1$

(ii) *For* $\alpha > 0.217234$, *there is only one fixed point* $O(0,\ 0)$ *being the center.*

(iii) *For* $\alpha = 0.217234$, *there are three fixed points:* $O(0,\ 0)$ *being the center and* $C_1(x_0,\ 0)$ *and* $C_2(-x_0,\ 0)$ *being bifurcation points with two zero eigenvalues, where* x_0 *is the positive root of equation* $\sin x = -\alpha x$.

(iv) *For* $0 < \alpha < 0.217234$, *there are five fixed points in the internal* $(-2\pi,\ 2\pi)$: $O(0,\ 0)$ *being the center,* $C_1(x_1,\ 0)$ *and* $C_3(-x_1,\ 0)$ *being saddles, and* $C_2(x_2,\ 0)$ *and* $C_4(-x_2,\ 0)$ *being centers, where* x_1 *and* x_2 *are the positive roots of equation* $\sin x = -\alpha x$ *in the internals* $(\pi, 3\pi/2)$ *and* $(3\pi/2,\ 2\pi)$, *respectively.*

(v) *For* $-1 < \alpha < 0$, *there are three fixed points in the internal* $(-2\pi,\ 2\pi)$: $O(0,\ 0)$ *being the center,* $C_1(x_1,\ 0)$ *and* $C_3(-x_1,\ 0)$ *being saddles, where* x_1 *is the positive root of equation* $\sin x = -\alpha x$ *in the internal* $(0,\ \pi)$, *respectively.*

(vi) *For* $\alpha = -1$, *there is only one fixed point:* $O(0,\ 0)$ *being bifurcation points with two zero eigenvalues.*

(vii) For $\alpha < -1$, *there is only one fixed point:* $O(0,\ 0)$ *being the saddle.*

Figure 1a and b gives the phase portraits for $\alpha = 0$ and $\alpha = 0.1(\alpha < \alpha_0)$, respectively. From Fig. 1a and b, we observe that the fixed points $(x_1, 0)$ and $(-x_1, 0)$ are connected by two heteroclinic orbits Γ^+_{het} and Γ^-_{het}, $(x_1, 0)$ is connected to itself by homoclinic orbit Γ^+_{hom}, and $(-x_1, 0)$ is connected to itself by homoclinic orbit Γ^-_{het}.

In the following sections, we use Melnikov methods to study how to change the dynamics of unperturbed system (2) under the periodic perturbations and how to suppress the chaotic dynamics by adjusting parametric excitation for $0 < \alpha < \alpha_0$.

3 Chaos inhibition conditions

By Lemma 1(iv) and Fig. 1b, we only consider the perturbed system (1) for $0 < \alpha < \alpha_0$. By using the Melnikov methods proposed in [7], we will give the criteria for controlling homoclinic and heteroclinic chaos, respectively.

The Melnikov function for system (1) can be given by

$$M(t_0) = \int_{-\infty}^{+\infty} y_0(t)\{f_1 \sin[\omega(t+t_0)+\theta] - f_0 \cos[\Omega(t+t_0)+\Psi] \sin x_0(t)\}\mathrm{d}t - \delta \int_{-\infty}^{+\infty} y_0^2(t)\mathrm{d}t, \tag{5}$$

where $(x_0,\ y_0) = (x_0(t),\ y_0(t))$ is the unperturbed homoclinic or heteroclinic orbits.

We first compute Melnikov function for the homoclinic orbits. Because $y_0(t)$ is odd and $x_0(t)$ is even in this case, by simple calculation, Melnikov function (5) becomes

$$\begin{aligned} M_1(t_0) &= -2\delta \int_0^{\infty} y_0^2(t)\mathrm{d}t \\ &\quad + 2f_1 \cos(\omega t_0 + \theta) \int_0^{\infty} y_0 \sin(\omega t)\mathrm{d}t \\ &\quad + 2f_0 \sin(\Omega t_0 + \Psi) \int_0^{\infty} y_0(t) \sin(\Omega t) \sin[x_0(t)]\mathrm{d}t \\ &= -C_{\text{hom}} + A_{\text{hom}} \cos(\omega t_0 + \theta) \\ &\quad + B_{\text{hom}} \sin(\Omega t_0 + \Psi), \end{aligned} \tag{6}$$

where $C_{\mathrm{hom}} = 2\delta \int_0^\infty y_0^2(t)\mathrm{d}t$ is a constant once $y_0(t)$ is given,

$$A_{\mathrm{hom}} = 2f_1 \int_0^\infty y_0(t)\sin(\omega t)\mathrm{d}t$$

and

$$B_{\mathrm{hom}} = 2f_0 \int_0^\infty y_0(t)\sin(\Omega t)\sin[x_0(t)]\mathrm{d}t$$

are functions of the frequencies Ω and ω, respectively.

For the heteroclinic orbits, $y_0(t)$ is even and $x_0(t)$ is odd. Thus Melnikov function (5) can be simplified as

$$M_2(t_0) = -C_{\mathrm{het}} + A_{\mathrm{het}}\sin(\omega t_0 + \theta) + B_{\mathrm{het}}\sin(\Omega t_0 + \Psi), \tag{7}$$

where

$$C_{\mathrm{het}} = 2\delta \int_0^\infty y_0^2(t)\mathrm{d}t, \quad A_{\mathrm{het}} = 2f_1 \int_0^\infty y_0(t)\cos(\omega t)\mathrm{d}t$$

and

$$B_{\mathrm{het}} = 2f_0 \int_0^\infty y_0(t)\sin(\Omega t)\sin[x_0(t)]\mathrm{d}t.$$

Let $t_1 = t_0 + \theta/\omega$ and $\phi = \Psi - \theta\Omega/\omega$, then Melnikov function (6) and (7) become

$$M_1(t_1) = -C_{\mathrm{hom}} + A_{\mathrm{hom}}\cos(\omega t_1) + B_{\mathrm{hom}}\sin(\Omega t_1 + \phi) \tag{8}$$

and

$$M_2(t_1) = -C_{\mathrm{het}} + A_{\mathrm{het}}\sin(\omega t_1) + B_{\mathrm{het}}\sin(\Omega t_1 + \phi), \tag{9}$$

respectively.

By the meaning of Melnikov functions, we can get the following results.

Theorem 1 *If $f_0 = 0$ and $A_{\mathrm{hom}} - C_{\mathrm{hom}} \geq 0$, then the homoclinic bifurcation of the system (1) will occur, which implies that the system (1) may be chaotic. If $f_0 \neq 0$ and $B_{\mathrm{hom}} \leq A_{\mathrm{hom}} - C_{\mathrm{hom}}$, then the homoclinic bifurcation of the system (1) will occur, which implies that the system (1) may be chaotic.*

Theorem 2 *If $f_0 = 0$ and $A_{\mathrm{het}} - C_{\mathrm{het}} \geq 0$, then the heteroclinic bifurcation of the system (1) will occur, which implies that the system (1) may be chaotic. If $f_0 \neq 0$, $A_{\mathrm{het}} - C_{\mathrm{het}} \geq 0$ and $B_{\mathrm{het}} \leq A_{\mathrm{het}} - C_{\mathrm{het}}$, then the heteroclinic bifurcation of the system (1) will occur, which implies that the system (1) may be chaotic.*

According to Theorem 1 and Theorem 2, we obtain that a necessary condition for $M_1(t_1)$ or $M_2(t_1)$ always having the same sign is $B_{\mathrm{hom}} > A_{\mathrm{hom}} - C_{\mathrm{hom}}$ for (8) or $B_{\mathrm{het}} > A_{\mathrm{het}} - C_{\mathrm{het}} \geq 0$ for (9). Because of the symmetry of homoclinic and heteroclinic orbits, they will give rise to the same set of optimal initial phase-difference that are suitable for taming the chaotic dynamics. By optimal suppressing values of ϕ (denoted as ϕ_{opt}), we can obtain the optimal suppressing values of Ψ (denoted as Ψ_{opt}).

4 Suitable initial phase-difference intervals

In this section, we investigate the ranges of suitable initial phase-difference intervals for chaos suppression by studying the changes of behavior of the Melnikov function (8) and (9). We shall consider the cases associated with the heteroclinic and homoclinic chaos separately. We always assume $\Omega/\omega = p/1,\ p \in N^+$.

4.1 For homoclinic orbits

If $f_0 = 0$, the chaos-suppressing excitation is eliminated. The corresponding Melnikov function

$$M_1'(t_1) = -C_{\mathrm{hom}} + A_{\mathrm{hom}}\cos(\omega t_1) \tag{10}$$

changes sign at some t_1, i.e., $C_{\mathrm{hom}} < A_{\mathrm{hom}}$. when we add the parametric excitation to the system (1), the sufficient condition for $M_1(t_1)$ change sign at some t_1 is $B_{\mathrm{hom}} \leq A_{\mathrm{hom}} - C_{\mathrm{hom}}$. Thus

$$B_{\mathrm{hom}} > A_{\mathrm{hom}} - C_{\mathrm{hom}} \equiv B_{\min} \tag{11}$$

is a necessary condition for $M_1(t_1)$ to always have the same sign.

In order to the maxima of $M_1'(t_1)$ coincide with the minima of $B_{\min}\sin(\Omega t_1 + \phi)$, we can get $\phi_{\mathrm{opt}} = 3\pi/2$ for the homoclinic orbits such that those functions are in opposition. Moreover, $\phi = \phi_{\mathrm{opt}} \pm \Delta\phi_{\max}$ is associated with the maximum deviation from ϕ_{opt} such that there still exists a value of $B_{\text{hom}}(B_{\text{hom}} > B_{\text{min}})$ for which $M_1(t_1) < 0,\ \forall t_1$. For $\phi > \phi_{\text{opt}} + \Delta\phi_{\max}$ or $\phi < \phi_{\text{opt}} - \Delta\phi_{\max}$, regulation is not expected. $\Delta\phi_{\max}$ is given by

$$\Delta\phi_{\max} = \arcsin\left\{\cos\left[p \cdot \arccos\left(\frac{C_{\text{hom}}}{A_{\text{hom}}}\right)\right]\right\}, \quad (12)$$

where $0 < p < \pi/(2\arccos(C_{\text{hom}}/A_{\text{hom}}))$. By the definition of ϕ, we get

$$\Psi_{\text{opt}} = \phi_{\text{opt}} + \frac{\Omega\theta}{\omega} = \frac{3\pi}{2} + \frac{\Omega\theta}{\omega} \quad (13)$$

and

$$\Delta\Psi_{\max} = \arcsin\left(\frac{C_{\text{hom}}}{A_{\text{hom}}}\right). \quad (14)$$

Next, we will study the dependence of the threshold values of f_0 on Ψ, specially on $\Psi = \Psi_{\text{opt}} \pm \Delta\Psi_{\max}$, regulation will only be effective when the lower threshold value of B_{hom}, hereafter denoted by $B^*_{\min}$ which is larger than $B_{\min}$ (which corresponds to $\Psi = \Psi_{\text{opt}}$). By simple calculation, we obtain the following analytical expression

$$B^*_{\min} = \frac{A_{\text{hom}} - C_{\text{hom}}}{\cos(\Delta\Psi_{\max})}. \quad (15)$$

For $\Psi = \Psi_{\text{opt}} \pm \Delta\Psi_{\max}$, the upper threshold values of B_{hom} (denoted as $B^*_{\max}$) is given by

$$B^*_{\max} = \frac{A_{\text{hom}}}{p^2}\cos(\Delta\Psi_{\max}), \quad (16)$$

for $\Omega = p\omega$. If $\Psi \notin [\Psi_{\text{opt}} - \Delta\Psi_{\max},\ \Psi_{\text{opt}} + \Delta\Psi_{\max}]$, chaos suppression is not guaranteed for any choice of B_{hom}.

Using (14), (15), and (16), we can get the following analytical expression of threshold values of f_0,

$$f_{0\min}(\Psi_{\text{opt}} \pm \Delta\Psi_{\max}) = \frac{f_1 R(1 - C_{\text{hom}}/A_{\text{hom}})}{\cos(\Delta\Psi_{\max})}, \quad (17)$$

$$f_{0\max}(\Psi_{\text{opt}} \pm \Delta\Psi_{\max}) = \frac{f_1 R}{p^2}\cos(\Delta\Psi_{\max}), \quad (18)$$

where $R = \int_0^{+\infty} y_0(t)\sin(\omega t)\mathrm{d}t / \int_0^{+\infty} y_0(t)\sin(\Omega t)\sin[x_0(t)]\mathrm{d}t$.

So, we can get the following conclusion.

Theorem 3 *Supposed the values of parameters α, δ, Ω, f_1, ω and θ are given. If $f_0 \in [f_{0min}(\Psi_{\text{opt}} \pm \Delta\Psi_{\max}), f_{0max}(\Psi_{\text{opt}} \pm \Delta\Psi_{\max})]$ and $\Psi \in [\Psi_{\text{opt}} - \Delta\Psi_{\max},\ \Psi_{\text{opt}} + \Delta\Psi_{\max}]$, then the homoclinic chaos of system (1) should be suppressed, where Ψ_{opt}, $\Delta\Psi_{\max}$, $f_{0min}(\Psi_{\text{opt}} \pm \Delta\Psi_{\max})$ and $f_{0max}(\Psi_{\text{opt}} \pm \Delta\Psi_{\max})$ are given in Eqs. (13), (14), (17) and (18), respectively.*

4.2 For heteroclinic orbits

For the heteroclinic orbits. let $t_1 = \tau_0 + \pi/2\omega$ and $\Phi = \phi + \Omega\pi/2\omega$, the function (9) can be changed into

$$M_2(\tau_0) = -C_{\text{het}} + A_{\text{het}}\cos(\omega\tau_0) + B_{\text{het}}\sin(\Omega\tau_0 + \Phi), \quad (19)$$

which show that the Melnikov functions of heteroclinic orbits and homoclinic orbits are similar. If Φ_{opt} is for (19), then $\phi_{\text{opt}} = \Phi_{\text{opt}} - \Omega\pi/2\omega$ is for (9). By definition of Φ_{opt}, we can obtain $\Phi_{\text{opt}} = 3\pi/2$, so $\phi_{\text{opt}} = 3\pi/2 - \Omega\pi/2\omega$, $\Psi_{\text{opt}} = \phi_{\text{opt}} + \Omega\theta/\omega$ for the heteroclinic orbits. We can obtain the following theorem in the same way.

Theorem 4 *Supposed the values of parameters α, δ, Ω, f_1, ω and θ are given. If $f_0 \in [f_{0min}(\Psi_{\text{opt}} \pm \Delta\Psi_{\max}), f_{0max}(\Psi_{\text{opt}} \pm \Delta\Psi_{\max})]$ and $\Psi \in [\Psi_{\text{opt}} - \Delta\Psi_{\max},\ \Psi_{\text{opt}} + \Delta\Psi_{\max}]$, then the heteroclinic chaos of system (1) should be suppressed, where $f_{0min}(\Psi_{\text{opt}} \pm \Delta\Psi_{\max}) = \frac{f_1 R(1 - C_{\text{het}}/A_{\text{het}})}{\cos(\Delta\Psi_{\max})}$, $f_{0max}(\Psi_{\text{opt}} \pm \Delta\Psi_{\max}) = \frac{f_1 R}{p^2}\cos(\Delta\Psi_{\max})$, $R = \frac{\int_0^{+\infty} y_0(t)\cos(\omega t)\mathrm{d}t}{\int_0^{+\infty} y_0(t)\sin(\Omega t)\sin[x_0(t)]\mathrm{d}t}$, $\Delta\Psi_{\max} = \arcsin(\frac{C_{\text{het}}}{A_{\text{het}}})$ and $\Psi_{\text{opt}} = 3\pi/2 - \Omega\pi/2\omega + \Omega\theta/\omega$.*

5 Numerical simulations

In this section, we give numerical simulation to check up the theoretical results obtained in the previous sections. Fixing $\alpha = 0.1$, $f_1 = 0.519$, $\delta = 0.125$, and other parameters are varied.

To check up our theoretical results, the homoclinic bifurcation curves for $A_{\text{hom}} = C_{\text{hom}}$ and heteroclinic bifurcation curve for $A_{\text{het}} = C_{\text{het}}$ plotted in $(\omega,\ f_1)$ plane are showed in Fig. 2, respectively. If $A_{\text{hom}} > C_{\text{hom}}$ or $A_{\text{het}} > C_{\text{het}}$, the system (1) may exhibit chaos at $f_0 = 0$. Taking $\omega = 1$, there are $R_1(\delta, \omega) = f_1 C_{\text{hom}}/A_{\text{hom}} = 0.2126$ and $R_2(\delta, \omega) =$

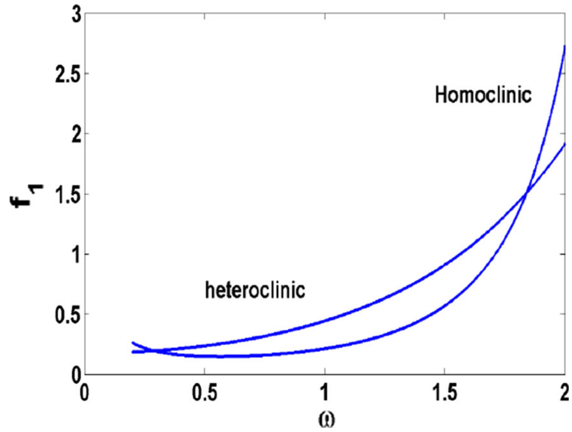

Fig. 2 Homoclinic bifurcation curve for $A_{\text{hom}} = C_{\text{hom}}$ and heteroclinic bifurcation curve for $A_{\text{het}} = C_{\text{het}}$ in (ω, f_1) plane with $\alpha = 0.1,\ \delta = 0.125$

$f_1 C_{\text{het}}/A_{\text{het}} = 0.4434$ in Fig. 2. Figure 3 show unstable (red) and stable (blue) manifolds associated with a saddle fixed point near (3.49906, 0) and (−3.49906, 0) for $\omega = 1$, $f_0 = 0$ and three values of f_1. For $f_1 = 0.2126$, Fig. 3a shows the unstable and stable manifolds of homoclinic orbits intersect tangentially, and the unstable and stable manifolds of heteroclinic orbits don't intersect. For $f_1 = 0.4434$, from Fig. 3b, we observe that the unstable and stable manifolds of homoclinic orbits intersect transversely, and the unstable and stable manifolds of heteroclinic orbits intersect tangentially. For $f_1 = 0.519$, the unstable and stable manifolds intersect transversely (Fig. 3c). When $\alpha = 0.1,\ \omega = 1,\ \delta = 0.125,\ f_1 = 0.519$, and $f_0 = 0$, the chaotic attractor is showed in Fig. 4. Now we add the parametric excitation in the chaos dynamics, the suppressing of heteroclinic chaos and the suppressing of homoclinic chaos are considered separately.

For the suppressing of heteroclinic chaos. Taking $\Omega = \omega = 1, \delta = 0.125$, and $f_1 = 0.519$, by Melnikov function (19), we have $\Phi_{\text{opt}} = 3\pi/2$, and by definition of Ψ_{opt}, we obtain $\Psi_{\text{opt}} = \pi + \pi/6$ and $\Delta\Psi_{\max} = 1.0242$ for the heteroclinic orbits. Thus, for Ψ_{opt} and $\Psi_{\text{opt}} \pm \Delta\Psi_{\max}$, the suitable intervals of f_0 for chaos control are approximately [0.0779 ,0.5349] and [0.1499,0.278], respectively.

The bifurcation diagram of (1) in (f_0, y) plane at $\Omega = \omega = 1,\ \delta = 0.125,\ f_1 = 0.519,\ \Psi = \Psi_{\text{opt}} = \pi + \frac{\pi}{6}$ and bifurcation diagram in (Ψ, y) plane at $\Omega = \omega = 1,\ \delta = 0.125,\ f_1 = 0.519,\ f_0 = 0.2$ are given in Fig. 5a, b, respectively. By Theorem 4, we obtain that the chaos in the interval [0.0779 ,0.5349] of f_0 for $\Psi = \Psi_{\text{opt}}$ and chaos in the interval

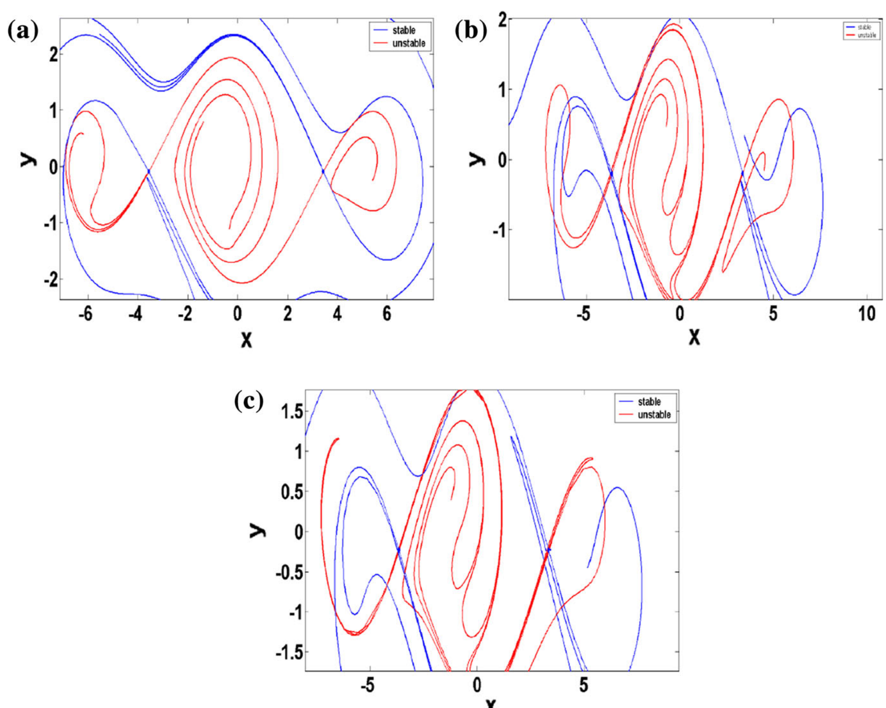

Fig. 3 Poincaré maps for system (1), showing stable and unstable manifolds of saddles for $\alpha = 0.1,\ \omega = 1,\ \delta = 0.125,\ f_0 = 0$ and several values of f_1: **(a)** for $f_1 = 0.2126$, **(b)** for $f_1 = 0.4434$, **(c)** for $f_1 = 0.5319$

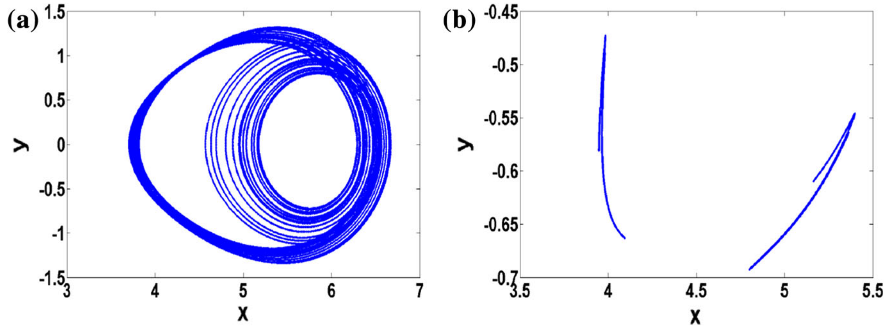

Fig. 4 The chaotic attractor of system (1) for $\alpha = 0.1,\ \omega = 1,\ \delta = 0.125,\ f_1 = 0.519$ and $f_0 = 0$: **a** Phase portrait; **b** Poincaré map

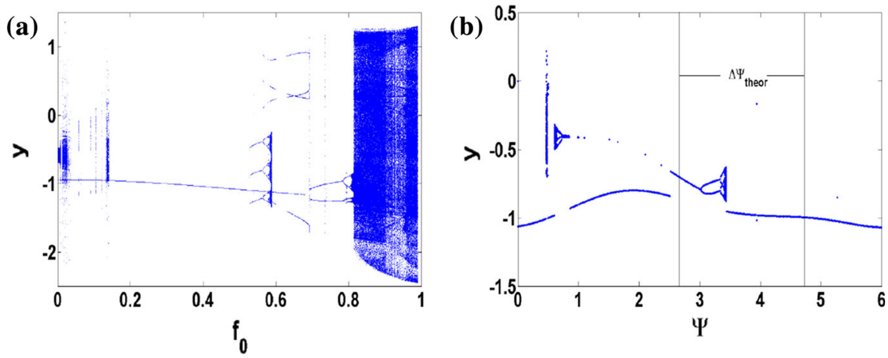

Fig. 5 Bifurcation diagrams of system (1) at $\alpha = 0.1,\ \delta = 0.125,\ \Omega = \omega = 1$ and $f_1 = 0.519$: (a) in (f_0, y) plane at $\Psi = \Psi_{\text{opt}} = \pi + \frac{\pi}{6}$; (b) in (Ψ, y) plane at $f_0 = 0.2$

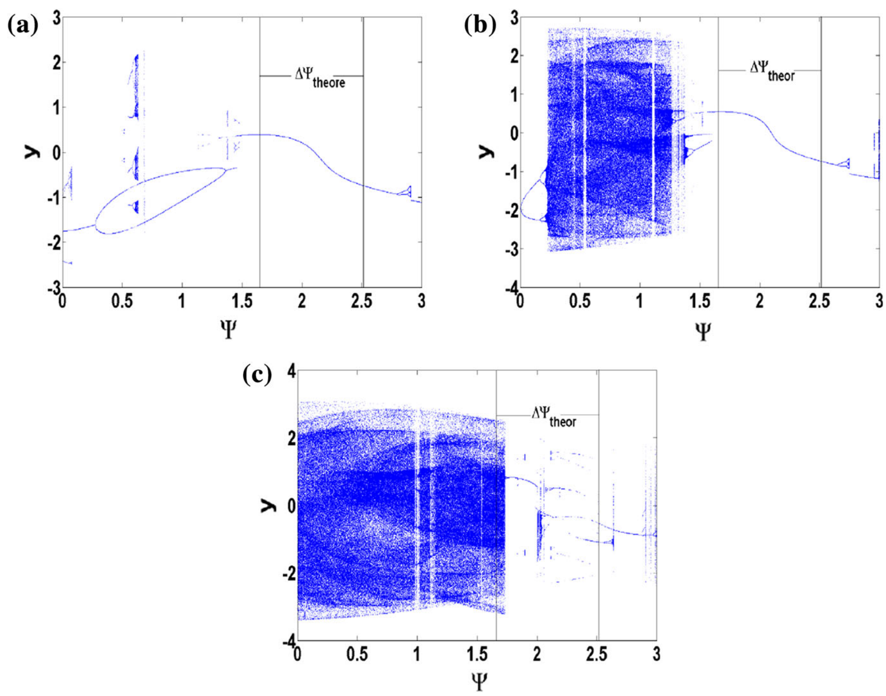

Fig. 6 Bifurcation diagram in (Ψ, y) plane of system (1) at $\alpha = 0.1,\ \delta = 0.125,\ \Omega = \omega = 1$ and $f_1 = 0.519$: (a) $f_0 = 0.75$; (b) $f_0 = 0.9$; (c) $f_0 = 1.4$

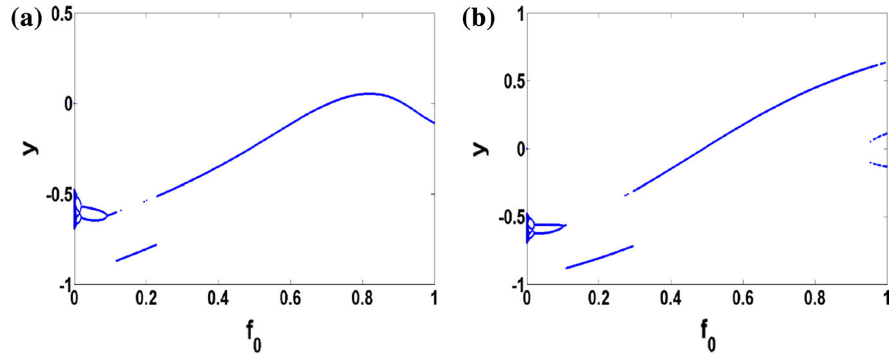

Fig. 7 Bifurcation diagram in (f_0, y) plane of system (1) at $\alpha = 0.1,\ \delta = 0.125,\ \Omega = \omega = 1$ and $f_1 = 0.519$: (a) $\Psi = \Psi_{\text{opt}}$; (b) $\Psi = \Psi_{\text{opt}} - \Delta\Psi_{\max}$

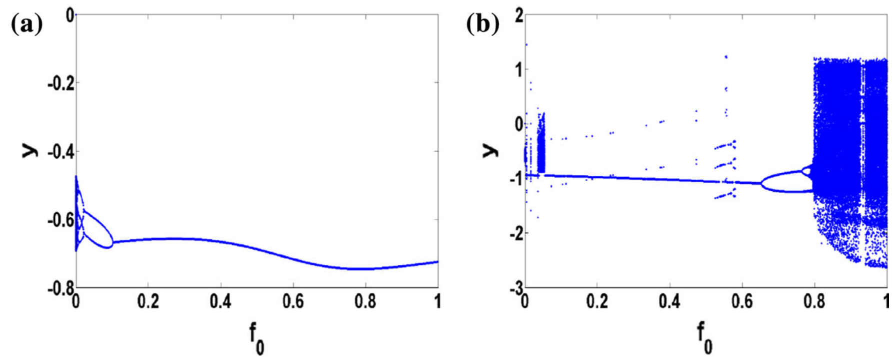

Fig. 8 Bifurcation diagram in (f_0, y) plane of system (1) at $\alpha = 0.1,\ \delta = 0.125,\ \Omega = \omega = 1$ and $f_1 = 0.519$: (a) $\Psi = \Psi_{\text{opt}} + \Delta\Psi_{\max}$; (b) $\Psi = 4$

$[\Psi_{\text{opt}} - \Delta\Psi_{\max}, \Psi_{\text{opt}} + \Delta\Psi_{\max}] = [2.641, 4.6894]$ for $f_0 \in [0.1499, 0.278]$ should be suppressed. In fact, we find that the chaostic behaviors in the subset of above intervals can be controlled to periodic behaviors, which indicate the numerical obtained ranges of suppression for heteroclinic chaos are less than the theoretical predictions.

For the suppressing of homoclinic chaos. Taking $\Omega = \omega = 1, \delta = 0.125, f_1 = 0.519$, by the Melnikov function (6), the definition of Ψ_{opt} and parameters values, we have $\Psi_{\text{opt}} = \frac{\pi}{2} + \frac{\pi}{6},\ \Delta\Psi_{\max} = 0.422$. Thus, for $\Psi = \Psi_{\text{opt}}$ and $\Psi_{\text{opt}} \pm \Delta\Psi_{\max}$, the interval of suitable of f_0 for chaos control is approximately (0.6277, 1.0631] and (0.6881, 0.9698].

The maximum range of f_0 for Ψ_{opt} is (0.6277,1.0631], the theoretical range of Ψ is $[\Psi_{\text{opt}} - \Delta\Psi_{\max}, \Psi_{\text{opt}} + \Delta\Psi_{\max}] \approx [1.6724, 2.5164]$. Figure 6a–c corresponds to the cases $f_0 = 0.75,\ 0.9$ and 1.4, respectively. Figure 6a, b shows the theoretical ranges of $\Delta\Psi_{\max}$ are less than the numerically obtained ranges of suppression of chaos, and the chaotic motions can be controlled to period-1 orbit by adjusting parameter Ψ. Note that, although suppression of homoclinic chaos is not expected at $f_0 = 1.4$, the system (1) can also reach periodic states by adjusting parameter Ψ.

The bifurcation diagrams corresponding to $\Psi = \Psi_{\text{opt}},\ \Psi = \Psi_{\text{opt}} \pm \Delta\Psi_{\max}$, and $\Psi = 4$ are plotted in Fig. 7a, b, 8a and b, respectively. From the figures, we can see that the numerically obtained ranges of suppression of chaos for $\Psi = \Psi_{\text{opt}}$ and $\Psi = \Psi_{\text{opt}} \pm \Delta\Psi_{\max}$ are larger than those predicted theoretically. Moreover, for $\Psi = 4 \notin [\Psi_{\text{opt}} - \Delta\Psi_{\max}, \Psi_{\text{opt}} + \Delta\Psi_{\max}]$, suppression of homoclinic chaos is not expected.

For $\alpha = 0.1,\ d = 0.125,\ \Omega = \omega = 1,\ f_1 = 0.519,\ \theta = \frac{\pi}{6}$, the distribution (grid of 200×100 points) of maximum LEs plotted in $(\Psi/\pi,\ f_0)$ plane is shown in Fig. 9a. The local amplification (grid of 200×100 points) of Fig. 9a in the region $\Psi \in [\pi/2 + \pi/6 - \pi/4, \pi/2 + \pi/6 + \pi/4]$, $f_0 \in [0, 1.2]$ is given in Fig. 9b. For parameters f_0 and Ω, we find that the theoretical prediction regions of suppression chaos for homoclinic orbits is less than those in Fig. 9. For the heteroclinic orbits, we find that the region of chaos suppressing is less than the theoretical prediction. This indicate the suppression of homoclinic chaos is more effective than heteroclinic chaos.

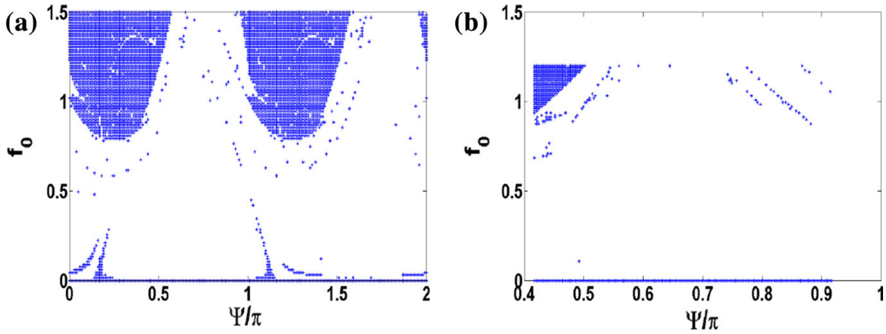

Fig. 9 (a) Maximum Lyapunov exponents (L) distribution in the (Ψ, f_0) parameter plane (grid of 200×100 points) for system (1) at $\alpha = 0.1$, $d = 0.125$, $\Omega = \omega = 1$, $f_1 = 0.519$. Where blue and white indicate that $L > 0$ and $L \leq 0$, respectively. (b)Local amplification of (a) in the region $\Psi \in [\frac{\pi}{2} + \frac{\pi}{6} - \frac{\pi}{4}, \frac{\pi}{2} + \frac{\pi}{6} + \frac{\pi}{4}]$ and $f_0 \in [0, 1.2]$

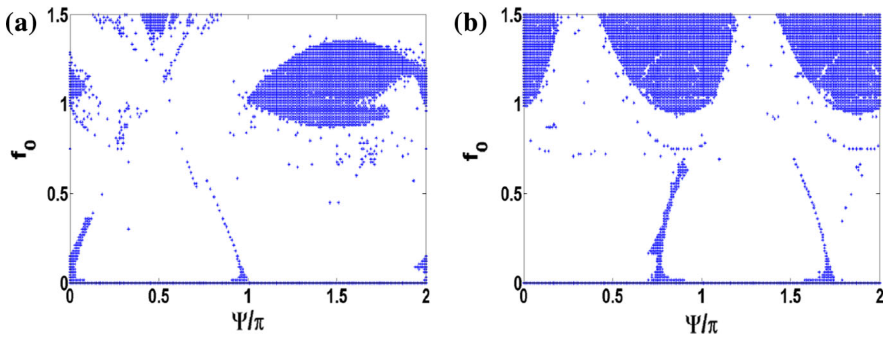

Fig. 10 Maximum Lyapunov exponents (L) distribution in the (Ψ, f_0) parameter plane (grid of 200×100 points) for system (1) at $\alpha = 0.1$, $d = 0.125$, $\omega = 1$, $f_1 = 0.519$, $\theta = \frac{\pi}{6}$. Where blue and white indicate that $L > 0$ and $L \leq 0$, respectively. (a) $\Omega = 2\omega$; (b) $\Omega = 3\omega$

Fig. 11 Bifurcation diagram in (f_0, y) plane of system (1) at $\alpha = 0.1$, $\delta = 0.125$, $\Omega = \omega = 1$, $\theta = \frac{\pi}{6}$ and $f_1 = 0.519$: **a** $\Omega = \frac{3\omega}{2}$, $\Psi = \frac{\pi}{2} + \frac{\pi}{6}$; **b** $\Omega = 2\omega$, $\Psi = \frac{\pi}{2} + \frac{\pi}{6}$

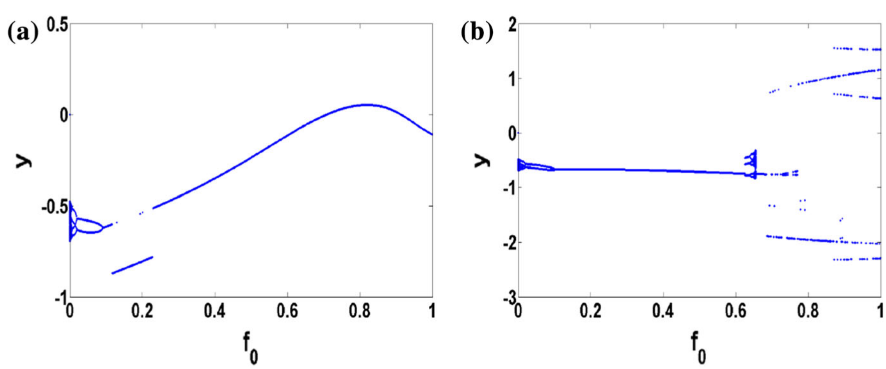

For the cases $\Omega = p\omega$, $(p > 1)$, we only plot the maximum LEs for $\Omega = 2\omega$ and $\Omega = 3\omega$. The maximum LEs of system (1) in (Ψ, f_0) plane (grid of 200×100 points) for $\alpha = 0.1$, $d = 0.125$, $\omega = 1$, $f_1 = 0.519$, $\Omega = 2\omega$ and $\alpha = 0.1$, $d = 0.125$, $\omega = 1$, $f_1 = 0.519$, $\theta = \pi/6$, $\Omega = 3\omega$ are shown in Fig. 10a and b, respectively. In each case, we observe that there is a wide region, in which homoclinic chaos can be suppressed.

In order to illustrate the influence of the phase-difference on inhibiting homoclinic chaos. The bifurcation diagrams for $\Omega = 3\omega/2$, $\Psi = \pi/2 + \pi/6$ and

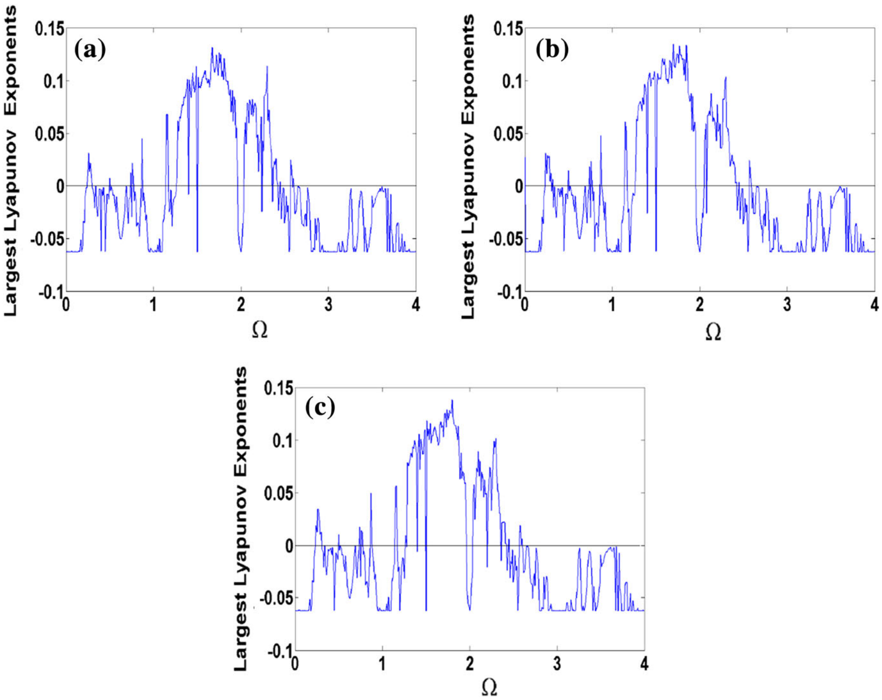

Fig. 12 Maximum Lyapunov exponents plotted against the frequency of perturbation of system (1) at $a = 0.1,\ \delta = 0.125,\ \omega = 1,\ f_1 = 0.519$ and $f_0 = 0.6$: (a) $\Psi = 0$; (b) $\Psi = \pi/2$; (c) $\Psi = \pi$

$\Omega = 2\omega$, $\Psi = \pi/2 + \pi/6$ are plotted in Fig. 11a and b, respectively. The diagrams show that there are wide ranges of f_0 in which chaotic motion can be converted to regular motion in each case. So, phase control is rather effective and can be used usually.

To know about the influence of the frequency of the chaos-suppressing excitation, we observe the change of the maximum LEs versus Ω. In Fig. 12a–c, we give the maximum LEs λ versus Ω for $\Psi = 0,\ \pi/2$, and π, respectively. As Ω trends to some resonant frequencies or in their neighbor, the value of the λ becomes negative and chaotic behaviors disappears. So if f_0 is chosen appropriately, the phase shift and frequency of the chaos-suppression excitation can play an important role in inhibiting chaos. So, the system chaotic motions can be converted to period-motions by adjusting the parameter f_0, for example, to period-one orbit as given in Figs. 7a, b, 8a, 11a, and b.

6 Conclusion

In this paper, we investigate the control of a chaotic pendulum system with excitations and a phase shift by using Melnikov methods, and give the chaos control conditions of heteroclinic bifurcation and homoclinic bifurcation, respectively. Numerical simulations show that the chaos behaviors can be controlled to periodic orbits, and the numerically obtained ranges of suppression for homoclinic chaos are larger than the theoretical predictions, and the numerically obtained ranges of suppression for heteroclinic chaos are less than the theoretical predictions. For chaos is not due to heteroclinic bifurcation and homoclinic bifurcation, although we can't give the condition of suppression of chaos using Melnikov methods, chaos also can be controlled by adjusting parameter of suppressing excitation.

Acknowledgments The authors would like to thank the reviewers for their helpful comments and suggestions. This work is supported by the National Natural Science Foundation of China (No. 11071066 and No. 11171206).

References

1. Alasty, A., Salarieh, H.: Nonlinear feedback control of chaotic pendulum in presence of saturation effect. Chaos Solitons Fractals **31**(2), 292–304 (2007)
2. Baker, G.L.: Control of the chaotic driven pendulum. Am. J. Phys. **63**(9), 832–838 (1995)
3. Cao, H.J., Chi, X.B., Chen, G.R.: Suppressing or inducing chaos by weak resonant excitations in an externally-forced froude pendulum. Int. J. Bifurc. Chaos **14**(3), 1115–1120 (2004)
4. Cao, H.J., Chen, G.R.: Global and local control of homoclinic and heteroclinic bifurcation. Int. J. Bifurc. Chaos **15**(8), 2411–2432 (2005)

5. Chacón, R.: Natural symmetries and regularization by means of weak parametric modulations in the forced pendulum. Phys. Rev. E **52**, 2330–2337 (1995)
6. Chacón, R.: General results on chaos suppression for biharmonically driven dissipative systems. Phys. Lett. A **257**, 293–300 (1999)
7. Chacón, R., Palmero, F., Balibrea, F.: Taming chaos in a driven Josephson junction. Int. J. Bifurc. Chaos **11**(7), 1897–1909 (2001)
8. Chacón, R.: Relative effectiveness of weak periodic excitations in suppressing homoclinic heteroclinic chaos. Eur. Phys. J. B **65**, 207–210 (2002)
9. Chen, G.R., Dong, X.: From Chaos to Order: Methodologies, Perspectives and Applications. World Scientific, Singapore (1998)
10. Chen, G.R., Moiola, J., Wang, H.O.: Bifurcation control: theories, methods and applications. Int. J. Bifurc. Chaos **10**(3), 511–548 (2000)
11. Chen, X., Fu, X., Jing, Z.: Complex dynamics in a pendulum equation with a phase shift. Int. J. Bifurc. **22**(12), 387–426 (2012)
12. D'Humieres, D., Beasley, M.R., Huberman, B.A., Libchaber, A.F.: Chaotic states and routes to chaos in the forced pendulum. Phys. Rev. A **26**(6), 3483–3492 (1982)
13. Jing, Z.J., Yang, J.P.: Complex dynamics in pendulum equation with parametric and external excitations (I). Int. J. Bifurc. Chaos **10**(16), 2887–2902 (2006)
14. Jing, Z.J., Yang, J.P.: Complex dynamics in pendulum equation with parametric and external excitations (II). Int. J. Bifurc. Chaos **10**(16), 3053–3078 (2006)
15. Kapitaniak, T.: Introduction. Chaos Solitons Fractals **15**, 201–203 (2003)
16. Lenci, S., Rega, G.: A procedure for reducing the chaotic response region in an impact mechanical system. Nonlinear Dyn. **15**, 391–409 (1998)
17. Lenci, S., Rega, G.: Optimal control of nonregular dynamics in a Duffing oscillator. Nonlinear Dyn. **33**, 71–86 (2003)
18. Lenci, S., Rega, G.: Optimal control of homoclinic bifurcation: theoretical treatment and practical reduction of safe basinerosion in the Helmholtz oscillator. J. Vib. Control **9**(3), 281–316 (2003)
19. Nayfeh, A.H., Mook, D.T.: Nonlinear Oscillations. Wiley, New York (1979)
20. Ott, E., Grebogi, N., Yorke, J.: Controlling chaos. Phys. Rev. Lett. **64**(11), 1196–1199 (1990)
21. Perira-Pinto, F.H.I., Ferreira, A.M., Savi, M.A.: Chaos control in a nonlinear pendulum using a semi-continuous method. Chaos Solitons Fractals **22**, 653–668 (2004)
22. Shinbrot, T., Ott, E., Grebogi, N., Yorke, J.: Using chaos to direct trajectories to targets. Phys. Rev. Lett. **65**, 3215–3218 (1990)
23. Wang, R.Q., Jing, Z.J.: Chaos control of chaotic pendulum system. Chaos Solitons Fractals **21**, 201–207 (2004)
24. Wiggins, S.: Global bifurcation and chaos: analytical methods. Springer, Berlin (1988)
25. Yagasaki, K., Uozumi, T.: Controlling chaos in a pendulum subjected to feedforward and feedback control. Int. J. Bifurc. Chaos **7**(12), 2827–2835 (1997)
26. Yagasaki, K.: Dynamics a pendulum subjected to feedforward and feedback control. JSME. Int. J. **41**(3), 545–554 (1998)
27. Yang, J.P., Jing, Z.J.: Inhibition of chaos in a pendulum equation. Chaos Solitons Fractals **35**, 726–737 (2008)